Abstract

This thesis covers two distinct topics: integral dispersion relations (IDRs) and ultra high energy cosmic ray (UHECR) anisotropy.
Many models of electroweak symmetry breaking predict new physics scales near LHC energies. Even if these particles are too massive to be produced on shell, it may be possible to infer their existence through the use of IDRs. Making use of Cauchy's integral formula and the analyticity of the scattering amplitude, IDRs are sensitive to changes in the cross section at all energies. We find that a sudden order one increase in the cross section can be detected well below the threshold energy. For two more physical models, the reach of the IDR technique is greatly reduced. The peak sensitivity for the IDR technique is shown to occur when the new particle masses are near the machine energy. Thus, IDRs do extend the reach of the LHC, but only to a window around $M_\chi \sim \sqrt{s_{\rm LHC}}$.
Determining anisotropies in the arrival directions of UHECRs ($\gtrsim 5\times10^{19}$ eV) is an important task in astrophysics. Spherical harmonics are a useful measure of anisotropy. The two lowest nontrivial spherical harmonics, the dipole and the quadrupole, are of particular interest, since they encapsulate a single source and a planar source. The best current UHECR experiments are all ground based, with highly nonuniform exposures which increases the complexity and error in inferring anisotropies. The two main advantages of space based observation of UHECRs are the increased field of view and the full sky coverage with uniform systematics. It turns out that there is an optimal latitude, which runs near the two largest experiments, for an experiment at which nonuniform exposure does not diminish the inference of the quadrupole moment. Consequently, assuming a quadrupole distribution, these experiments can reconstruct a quadrupole distribution to a high precision, without concern for their partial sky exposure. We then investigate the reach of a full sky experiment to detect anisotropies compared to these partial sky experiments. Simulations with dipoles and quadrupoles quantify the advantages of space based, all sky coverage.

Methods for Probing New Physics at High Energies

Peter B. Denton

Vanderbilt University Dissertation Defense

June 30, 2016

Work done with Tom J. Weiler.

1311.1248, Phys. Rev. D 89 (Feb, 2014) 035013

1409.0883, Astrophys. J. 802 no. 1, (2015) 25

1505.03922, JHEAp 8 (2015) 19

VANDERBILT

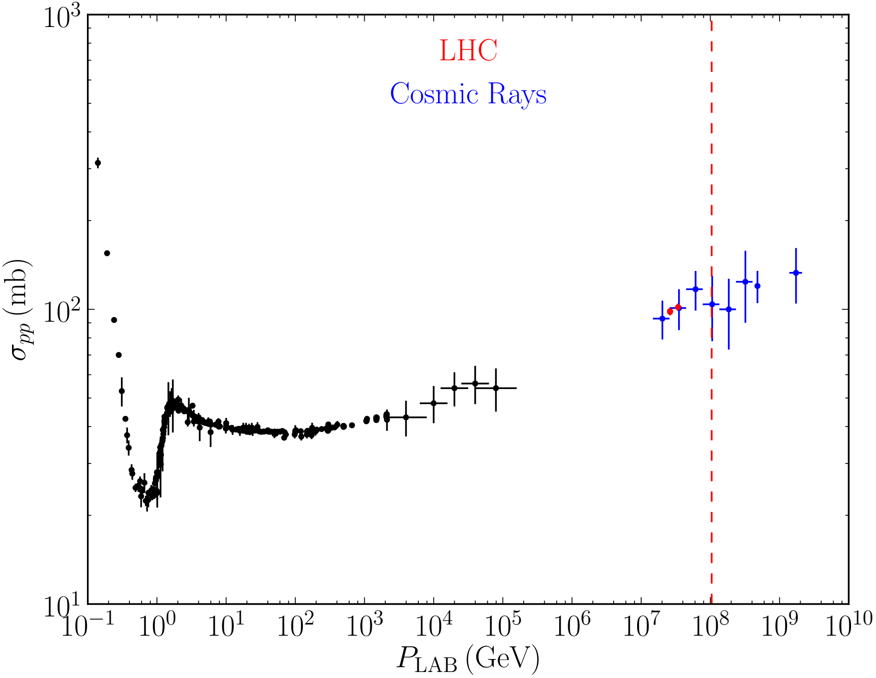
LHC
Cosmic Rays
σ_{pp} (mb)
10^3
10^2
10^1
10^{-1}
10^0
10^1
10^2
10^3
10^4
10^5
10^6
10^7
10^8
10^9
10^{10}
P_{LAB} (GeV)

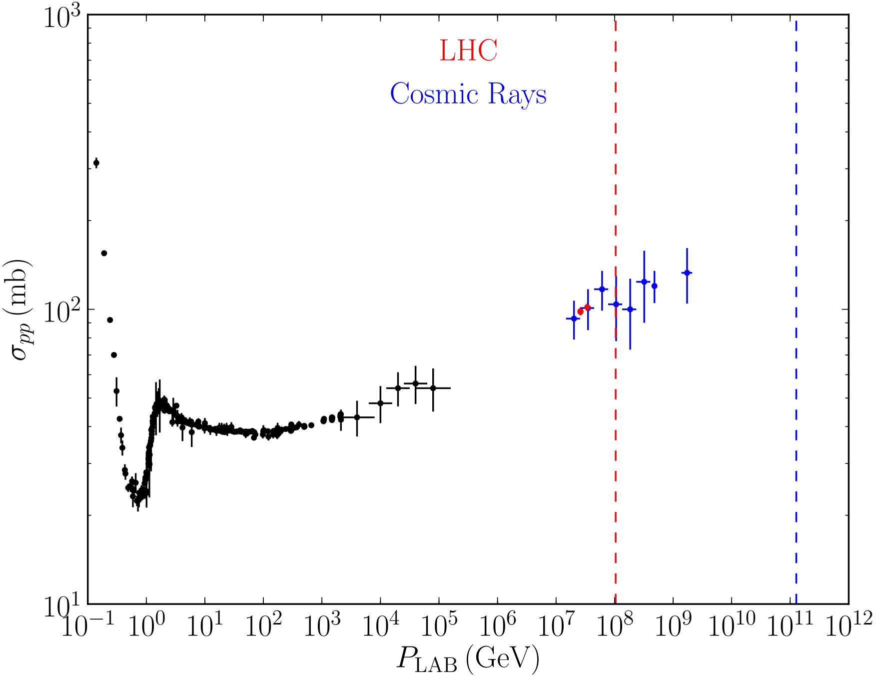

LHC
Cosmic Rays
σ_{pp} (mb)
10^3
10^2
10^1
10^{-1} 10^0 10^1 10^2 10^3 10^4 10^5 10^6 10^7 10^8 10^9 10^{10} 10^{11} 10^{12}
$P_{\rm LAB}$ (GeV)

Extending the Reach of the LHC with Integral Dispersion Relations

and

Ultra High Energy Cosmic Ray Anisotropies

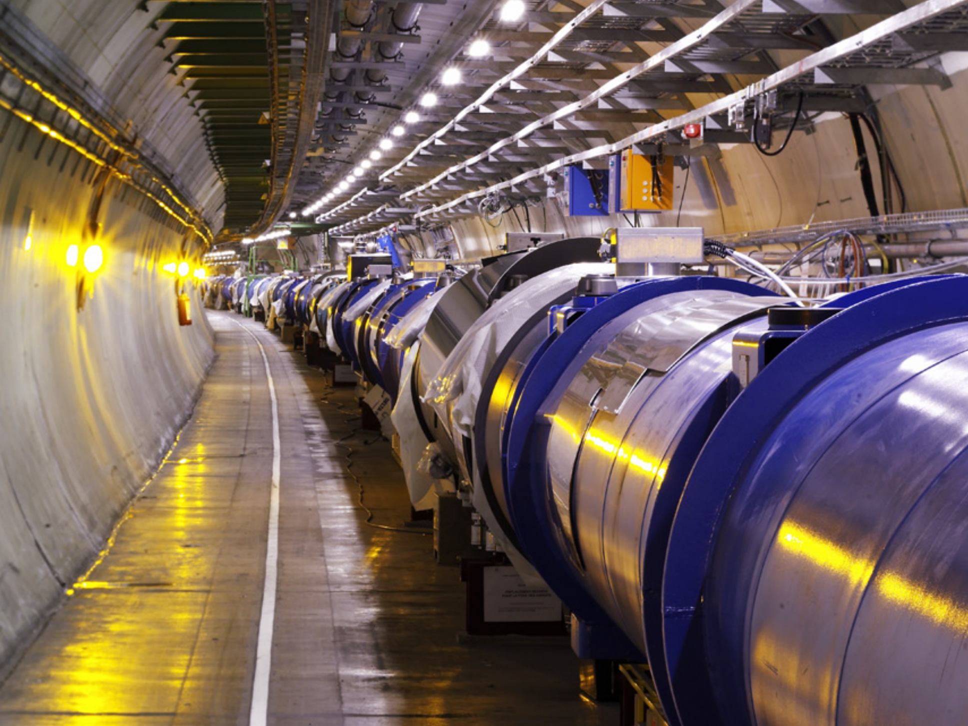

New Physics at the LHC

- Nobel prize for "old" physics found at the LHC.

2013 Nobel Prize to Englert, Higgs

Englert: PRL 13 (1964)

Higgs: PRL 13 (1964)

- Only hints of "new" (BSM) at the LHC yet.

ATLAS-CONF-2015-081

CMS-PAS-EXO-15-004

- New physics is typically constrained to $\lesssim$ few TeV.
- Suppose there is new physics near (above or below) 14 TeV...

Cross Section

- The cross section into a given direction is the amplitude squared,

$$\frac{d\sigma}{d\Omega} = |f|^2\,, \qquad f \in \mathbb{C}\,.$$

Cross Section

- The cross section into a given direction is the amplitude squared,

$$\frac{d\sigma}{d\Omega} = |f|^2\,, \qquad f \in \mathbb{C}\,.$$

- The optical theorem,

$$\sigma_{\rm tot} = \frac{4\pi}{p}\Im f(\theta = 0)\,.$$

Cross Section

- The cross section into a given direction is the amplitude squared,

$$\frac{d\sigma}{d\Omega} = |f|^2 , \qquad f \in \mathbb{C} .$$

- The optical theorem,

$$\sigma_{\rm tot} = \frac{4\pi}{p} \Im f(\theta = 0) .$$

- Define,

$$\rho(E) \equiv \frac{\Re f(E, \theta = 0)}{\Im f(E, \theta = 0)} .$$

Cross Section

- The cross section into a given direction is the amplitude squared,

$$\frac{d\sigma}{d\Omega} = |f|^2\,, \qquad f \in \mathbb{C}\,.$$

- The optical theorem,

$$\sigma_{\rm tot} = \frac{4\pi}{p}\Im f(\theta = 0)\,.$$

- Define,

$$\rho(E) \equiv \frac{\Re f(E, \theta = 0)}{\Im f(E, \theta = 0)}\,.$$

- Froissart bound,

$$\lim_{E\to\infty} \sigma_{\rm tot}(E) \le C \log^2\left(\frac{E}{E_0}\right)\,.$$

Froissart: Phys. Rev. 123 (1961)

Cauchy's Integral Formula

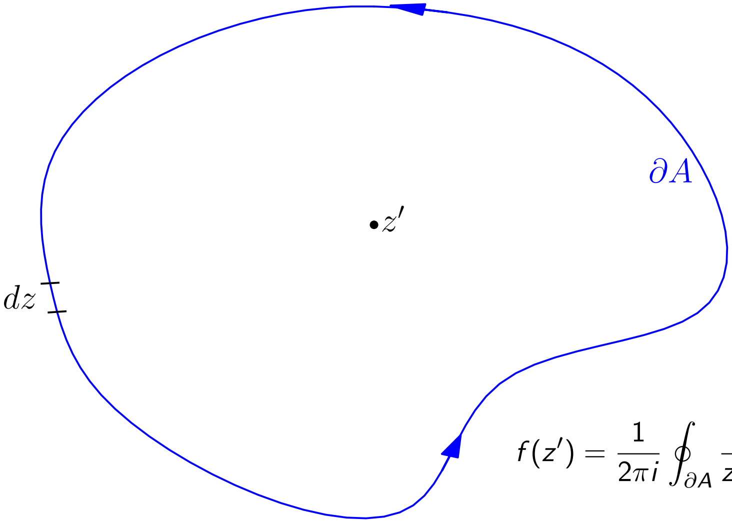

$$f(z') = \frac{1}{2\pi i}\oint_{\partial A}\frac{f(z)}{z-z'}dz$$

The Integral Dispersion Relation Contour

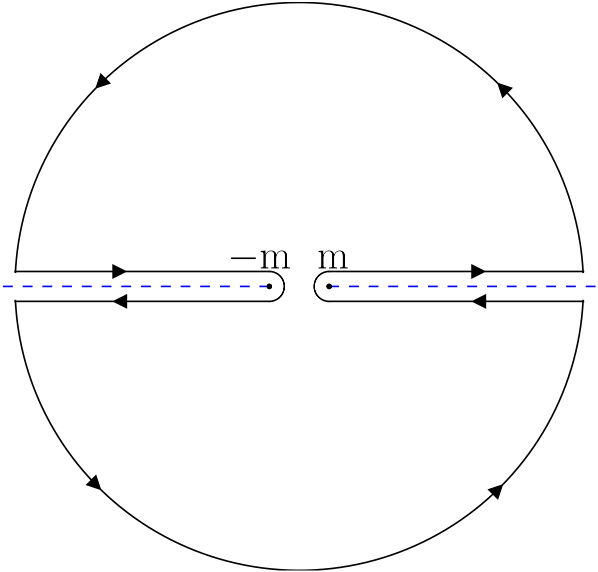

Integral Dispersion Relations

Subtraction + optical theorem,

$$\rho_{pp}(E)\sigma_{pp}(E) = \frac{4\pi}{p}\Re f(0) + \frac{E}{p\pi}\mathcal{P}\int_{m_p}^{\infty} dE'\,\frac{p'}{E'}\left[\frac{\sigma_{pp}(E')}{E'-E} - \frac{\sigma_{p\bar{p}}(E')}{E'+E}\right].$$

Block, Cahn: Rev. Mod. Phys. 57 (1985)

Integral Dispersion Relations

Subtraction + optical theorem,

$$\rho_{pp}(E)\sigma_{pp}(E) = \frac{4\pi}{p}\Re f(0) + \frac{E}{p\pi}\mathcal{P}\int_{m_p}^{\infty} dE' \frac{p'}{E'}\left[\frac{\sigma_{pp}(E')}{E'-E} - \frac{\sigma_{p\bar{p}}(E')}{E'+E}\right].$$

Block, Cahn: Rev. Mod. Phys. 57 (1985)

For integral to converge need $|\sigma_{pp} - \sigma_{p\bar{p}}| \to 0$.
Experimentally $|\sigma_{pp} - \sigma_{p\bar{p}}| \propto 1/\sqrt{E}$: fast enough (Pomeranchuk).

PDG: PRD 86 (2012)

Pomeranchuk: JETP 34 (1956)

Since $\lim_{E'\to\infty} \sigma(E')/E' \to 0$, outer circle $\to 0$.
From data, $f(0)$ is small (contributes < 1 part in 10^5 to ρ).

Block, Halzen: PRD 86 (2012)

Integral Dispersion Relations

Subtraction + optical theorem,

$$\rho_{pp}(E)\sigma_{pp}(E) = \frac{4\pi}{p}\Re f(0) + \frac{E}{p\pi}\mathcal{P}\int_{m_p}^{\infty} dE' \frac{p'}{E'}\left[\frac{\sigma_{pp}(E')}{E'-E} - \frac{\sigma_{p\bar{p}}(E')}{E'+E}\right].$$

Block, Cahn: Rev. Mod. Phys. 57 (1985)

For integral to converge need $|\sigma_{pp} - \sigma_{p\bar{p}}| \to 0$.
Experimentally $|\sigma_{pp} - \sigma_{p\bar{p}}| \overset{\propto}{\sim} 1/\sqrt{E}$: fast enough (Pomeranchuk).

PDG: PRD 86 (2012)

Pomeranchuk: JETP 34 (1956)

Since $\lim_{E'\to\infty} \sigma(E')/E' \to 0$, outer circle $\to 0$.
From data, $f(0)$ is small (contributes < 1 part in 10^5 to ρ).

Block, Halzen: PRD 86 (2012)

IDRs give ρ as a function of unknown high energy behavior.

Cross Section Modifications

- Consider modification of the general form,

$$\sigma(E) = \sigma_{\rm SM}(E)[1 + h(E)]\,,$$

where $h(E) = 0$ for $E < E_{\rm thr}$.

Cross Section Modifications

- Consider modification of the general form,

$$\sigma(E)=\sigma_{\rm SM}(E)[1+h(E)]\,,$$

where $h(E)=0$ for $E<E_{\rm thr}$.

- The simplest such modification is $h(E)=D\Theta(E-E_{\rm thr})$.

  That is, the cross section doubles at $E=E_{\rm thr}$ for $D=1$.

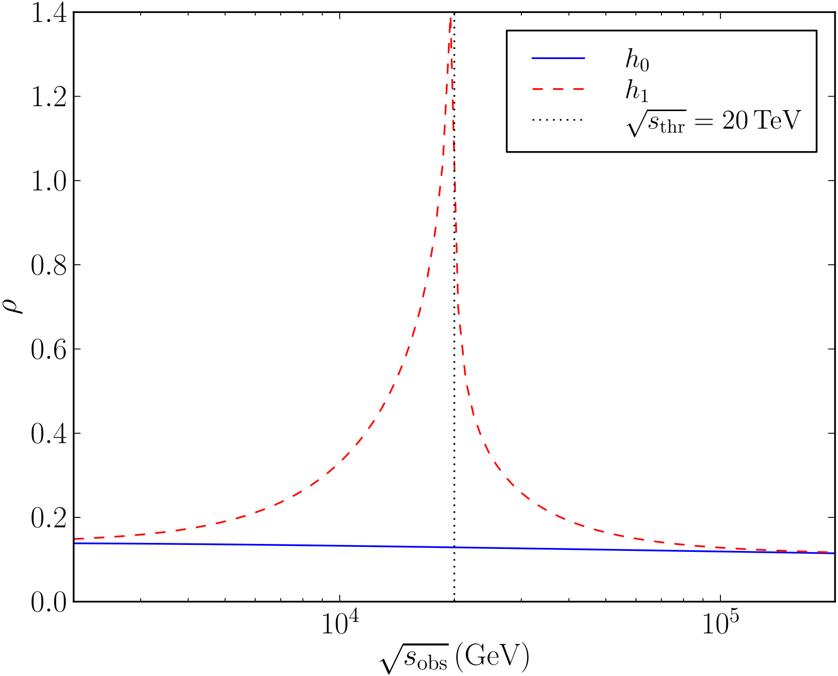

1.4
1.2
1.0
0.8
0.6
0.4
0.2
0.0
ρ
10^4
10^5
$\sqrt{s_{\rm obs}}$ (GeV)
h_0
h_1
$\sqrt{s_{\rm thr}} = 20$ TeV

Two Physical Models

Partonic Model

RPV SUSY: Replace one final state particle with a heavier partner.

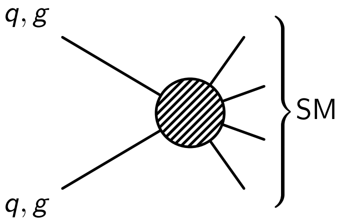

Wei et. al.: 1107.4461

Bazzocchi et. al.: 1202.1529

Bhattacherjee et. al.: 1301.2336

CMS: 1306.6643

CMS: 1310.3598

Partonic Model

RPV SUSY: Replace one final state particle with a heavier partner.

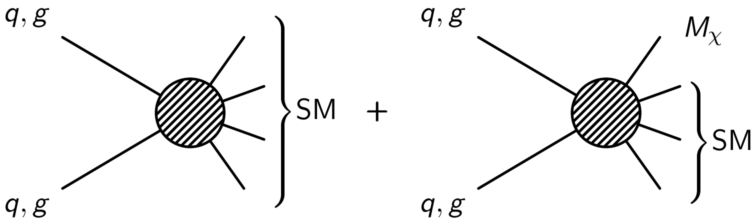

Wei et. al.: 1107.4461

Bazzocchi et. al.: 1202.1529

Bhattacherjee et. al.: 1301.2336

CMS: 1306.6643

CMS: 1310.3598

Partonic Model: h_2

We reduce the cross section by a phase space ratio given by

$$\sqrt{\frac{\lambda(\hat{s}, M_\chi^2, 0)}{\lambda(\hat{s}, 0, 0)}} = 1 - \frac{M_\chi^2}{\hat{s}}\,.$$

Partonic Model: h_2

We reduce the cross section by a phase space ratio given by

$$\sqrt{\frac{\lambda(\hat{s}, M_\chi^2, 0)}{\lambda(\hat{s}, 0, 0)}} = 1 - \frac{M_\chi^2}{\hat{s}}\,.$$

We integrate this in terms of the pdfs

$$h_2(s, M_\chi) = z \sum_{i,j} \int_{x_1 x_2 > M_\chi^2/s} dx_1 dx_2$$

$$\times f_i(x_1, M_\chi) f_j(x_2, M_\chi) x_1 x_2 \left(1 - \frac{M_\chi^2}{\hat{s}}\right)\,,$$

where $z = \sigma_{inel}/\sigma_{tot} \sim 0.7$.

CT10: 1302.6246

Diffractive Model: h_3

Cut final states into two blocks by pseudorapidity and we let M_X be the mass of the more massive one. Let $\xi \equiv M_X^2/s$.

$$\frac{d\sigma}{d\xi} = \frac{1+\xi}{\xi^{1+\epsilon}}\,, \qquad \epsilon \sim 0.08\,.$$

ATLAS: 1104.0326

Diffractive Model: h_3

Cut final states into two blocks by pseudorapidity and we let M_X be the mass of the more massive one. Let $\xi \equiv M_X^2/s$.

$$\frac{d\sigma}{d\xi} = \frac{1+\xi}{\xi^{1+\epsilon}}\,, \qquad \epsilon \sim 0.08\,.$$

ATLAS: 1104.0326

The bounds on the above integral change from SM $\to$ new physics,

$$h_3(s) = z\frac{1-2\epsilon+(\epsilon-1)\xi_\chi^{-\epsilon}+\epsilon\xi_\chi^{1-\epsilon}}{1-2\epsilon+(\epsilon-1)\xi_p^{-\epsilon}+\epsilon\xi_p^{1-\epsilon}}\Theta(1-\xi_\chi)\,,$$

$$\lim_{s\to\infty} h_3(s) = z\left(\frac{m_p}{M_\chi}\right)^{2\epsilon} \approx 0.23\left(\frac{1\,\mathrm{TeV}}{M_\chi}\right)^{2\epsilon}\,.$$

Total Cross Section Modifications

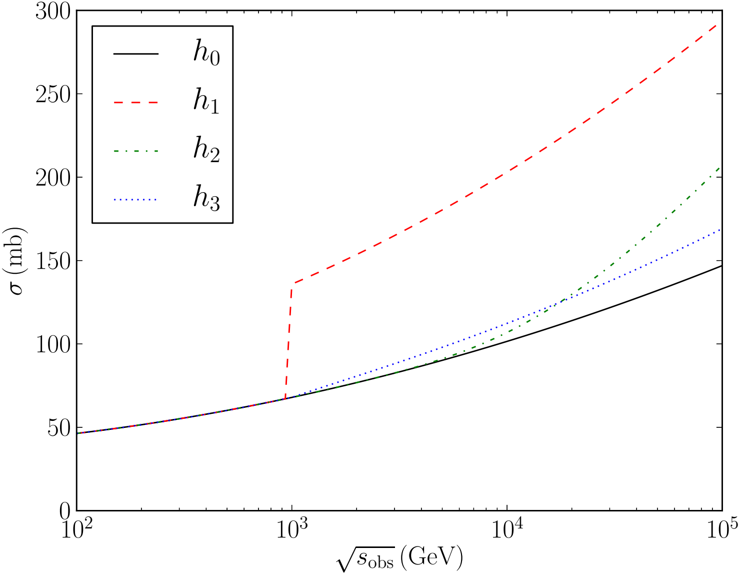

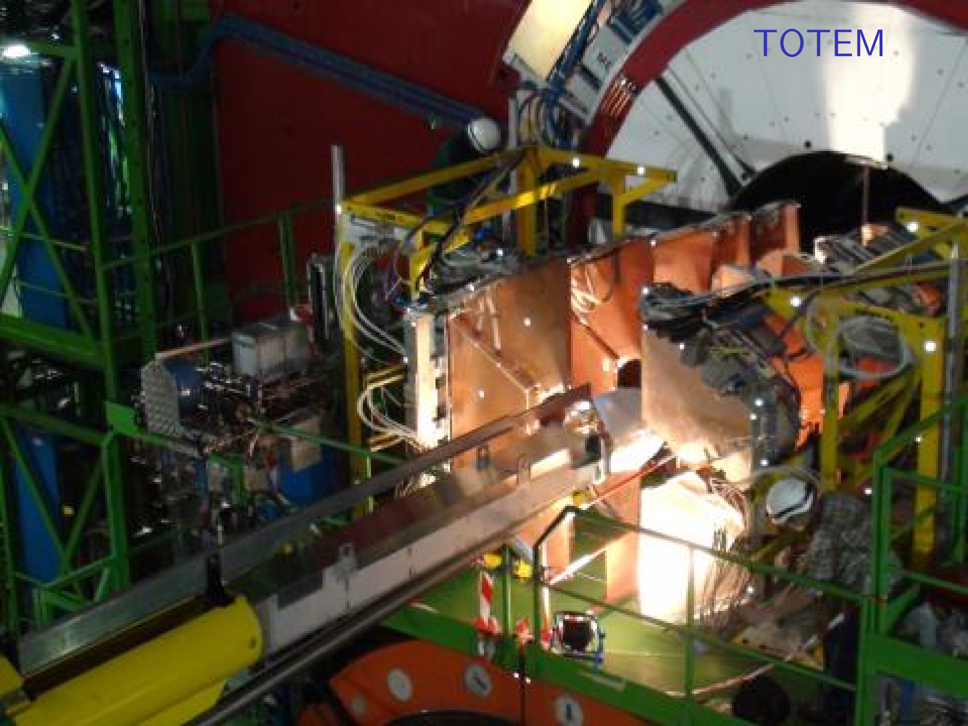
TOTEM

Experimental Status

ρ can be measured at the LHC with the experiment TOTEM.

- TOTEM: $\rho = 0.145$ at $\sqrt{s} = 7$ TeV (large errors).
- SM Prediction: $\rho = 0.1345$ at $\sqrt{s} = 7$ TeV.
- "Signal": $(\rho - \rho_{\rm SM})/\rho_{\rm SM} = 0.0781$ (a 0.1σ "signal").
- Excluded: $\rho > 0.32$ at 95%.

TOTEM: Europhys. Lett. 101 (2013)

Experimental Status

ρ can be measured at the LHC with the experiment TOTEM.

- TOTEM: $\rho = 0.145$ at $\sqrt{s} = 7$ TeV (large errors).
- SM Prediction: $\rho = 0.1345$ at $\sqrt{s} = 7$ TeV.
- "Signal": $(\rho - \rho_{\rm SM})/\rho_{\rm SM} = 0.0781$ (a 0.1σ "signal").
- Excluded: $\rho > 0.32$ at 95%.

TOTEM: Europhys. Lett. 101 (2013)

TOTEM gives the true value of ρ.

IDR Response at $\sqrt{s} = 7$ TeV for Step Function (h_1)

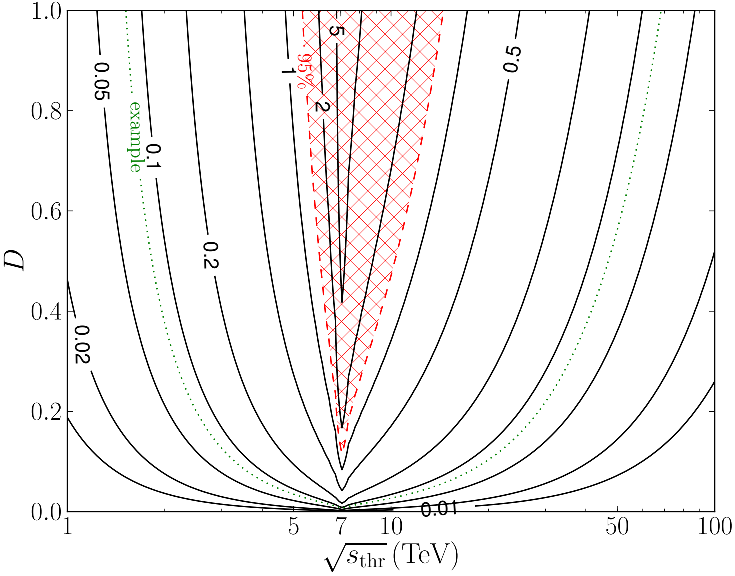

IDR Response at $\sqrt{s} = 7$ TeV for Parton Approach (h_2)

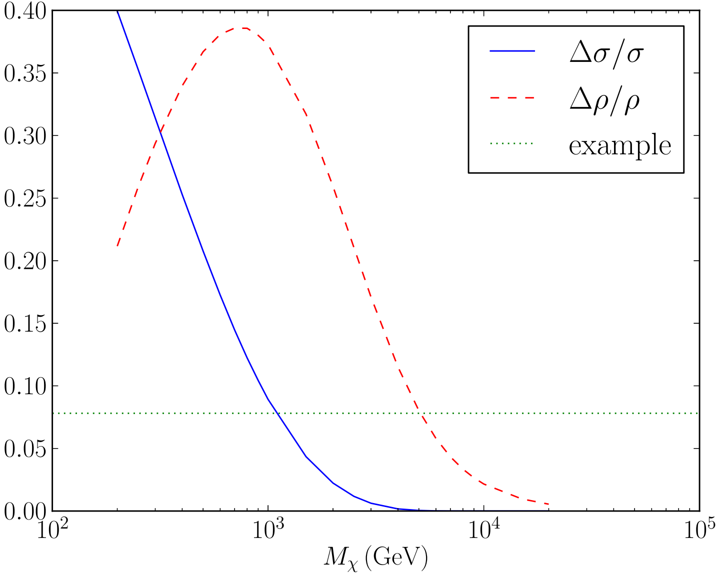

IDR Response at $\sqrt{s} = 7$ TeV for Diffractive Approach (h_3)

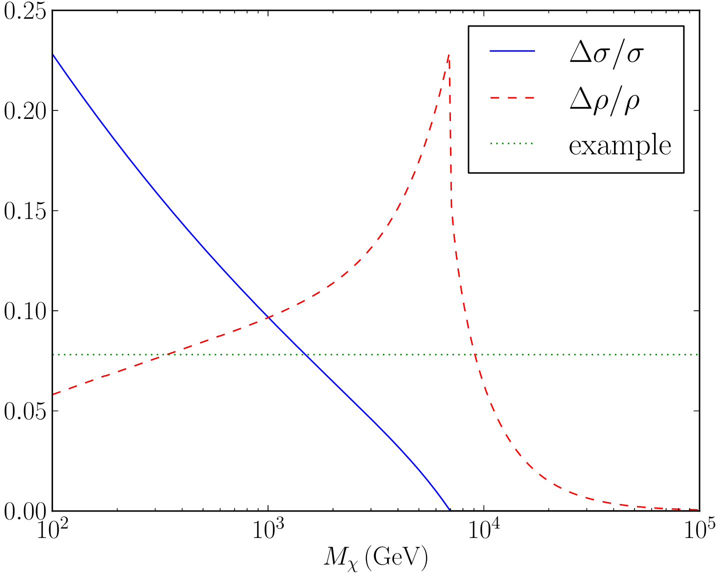

Integral Dispersion Relations: Conclusions

- IDRs can probe new physics in a largely model independent fashion.
- Most effective for new physics turning on near the machine energy.
- Await new data from future physics runs at the LHC.

Extending the Reach of the LHC with
Integral Dispersion Relations

and

Ultra High Energy Cosmic Ray Anisotropies

Highest Energy Particles in the Universe

Highest Energy Particles in the Universe

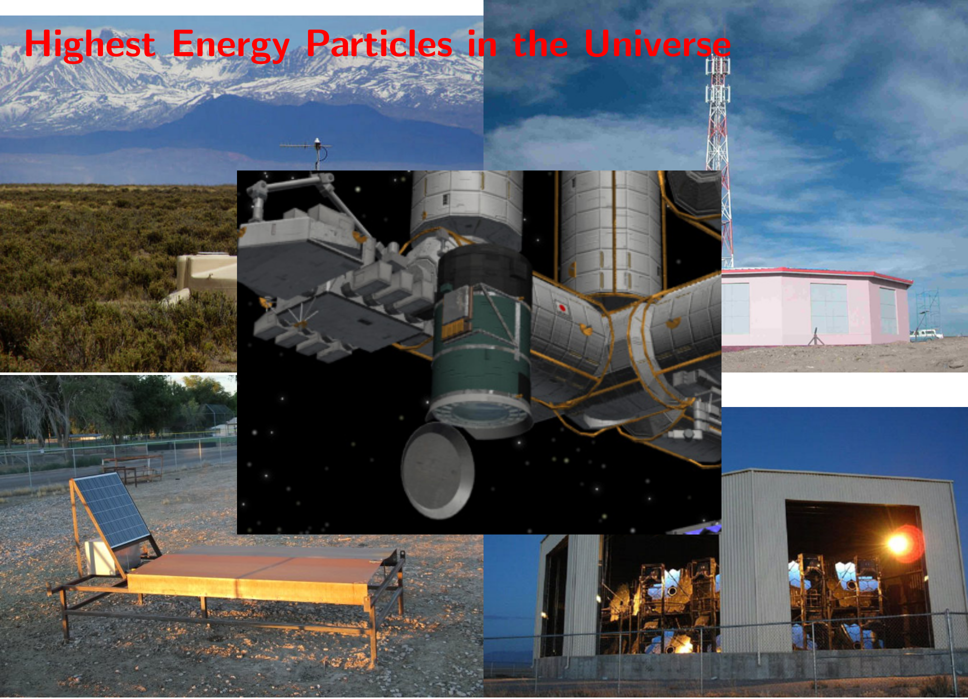

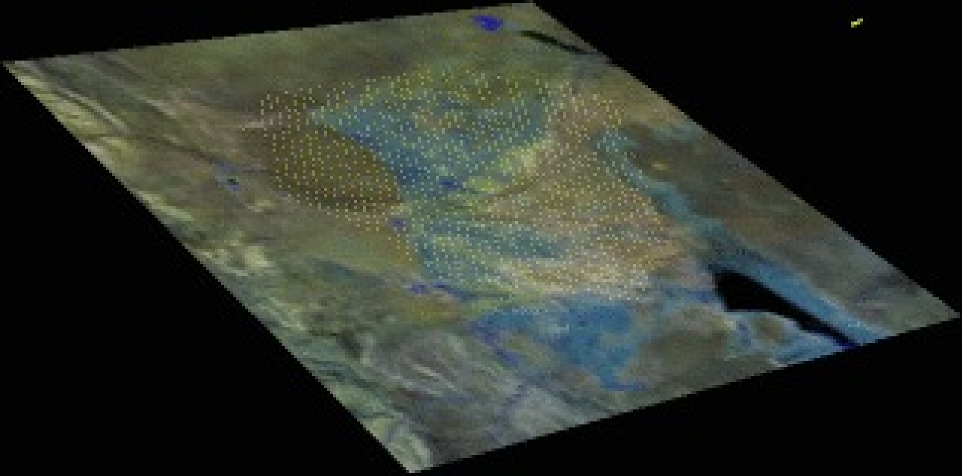

UHECR Anisotropy Unknowns

- How strong are the magnetic fields inside and between galaxies?

  Pshirkov et. al.: 1103.0814

  Jansson, Farrar: 1204.3662

- What is the composition of UHECRs? Protons? Iron nuclei?
- What is(are) the source(s) of UHECRs?
- How are UHECRs accelerated to such extreme energies?

  Gunn, Ostriker: PRL 22 (1969)

  Pruet, Guiles, Fuller: astro-ph/0205056

  Groves, Heckman, Kauffmann: astro-ph/0607311

  Fang, Kotera, Olinto: 1201.5197

- What is the cause of the end of the spectrum?

UHECR Anisotropy Knowns

- The magnetic field in the Milky Way cannot contain UHECRs.
- UHECRs with energies above ~ 50 EeV lose energy via the CMB.

Greisen: PRL 16 (1966)

Zatsepin, Kuzmin: JETP Lett. 4 (1966)

- UHECR sources must be close $\Rightarrow$ anisotropies.
- UHECRs bend in galactic and extragalactic magnetic fields.
- No conclusive anisotropies found yet.

UHECR Anisotropy

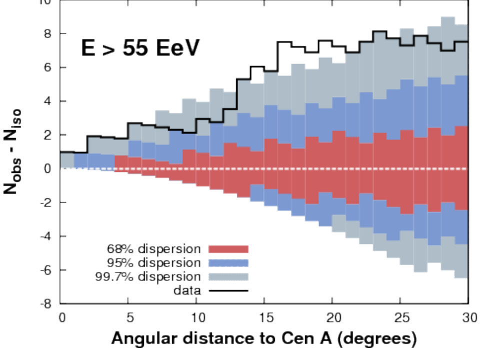

Auger: 1106.3048

UHECR Anisotropy

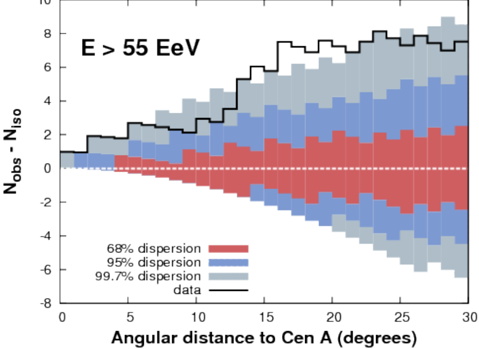

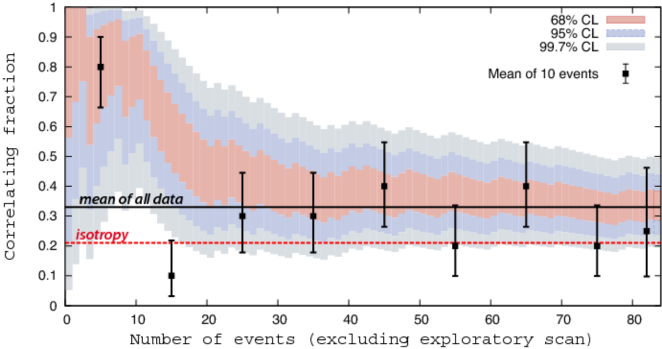

Auger: 1207.4823

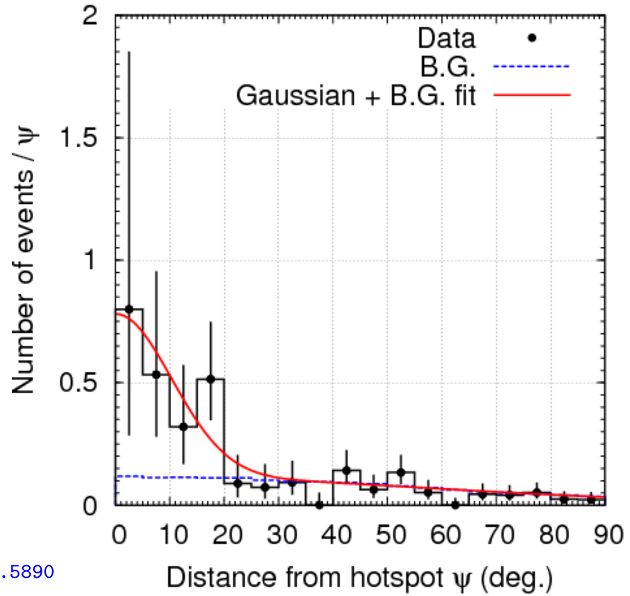
Data
B.G.
Gaussian + B.G. fit
Number of events / ψ
Distance from hotspot ψ (deg.)
0
0.5
1
1.5
2
0
10
20
30
40
50
60
70
80
90

TA: 1404.5890

Spherical Harmonics: Distributions on the Sky

- General structure can be quantified in terms of Y_ℓ^m's which provide an orthogonal expansion of the sky.
- The true distribution of UHECRs as seen at earth follows

$$I(\Omega) = \sum_{\ell,m} a_\ell^m Y_\ell^m(\Omega) \,.$$

All of the information is encoded in the a_ℓ^m.

- The power spectrum is rotational invariant.

$$C_\ell = \frac{1}{2\ell+1} \sum_m |a_\ell^m|^2 \,.$$

Spherical Harmonics Visualizations

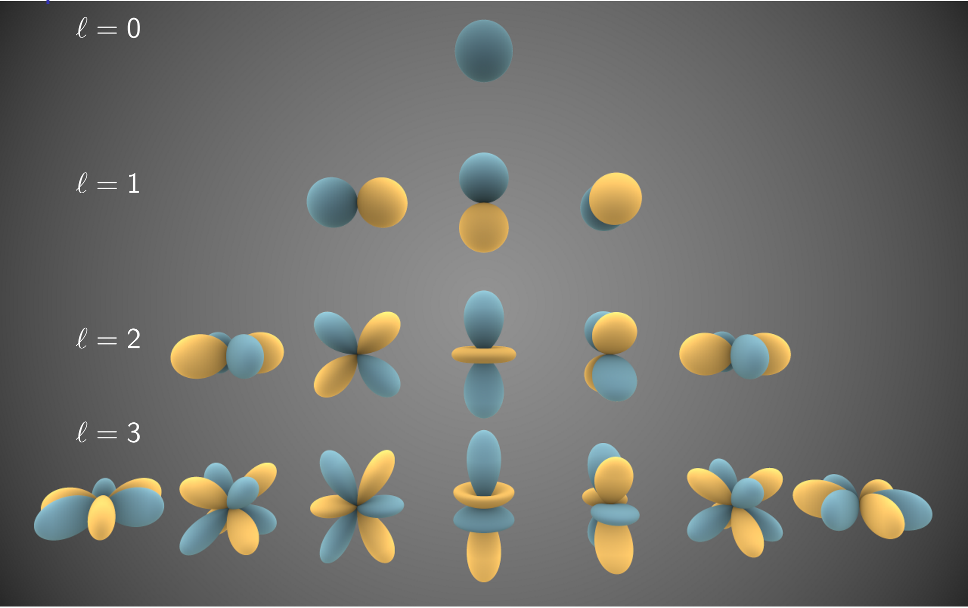

en.wikipedia.org/wiki/Spherical_harmonics

Sample Dipole

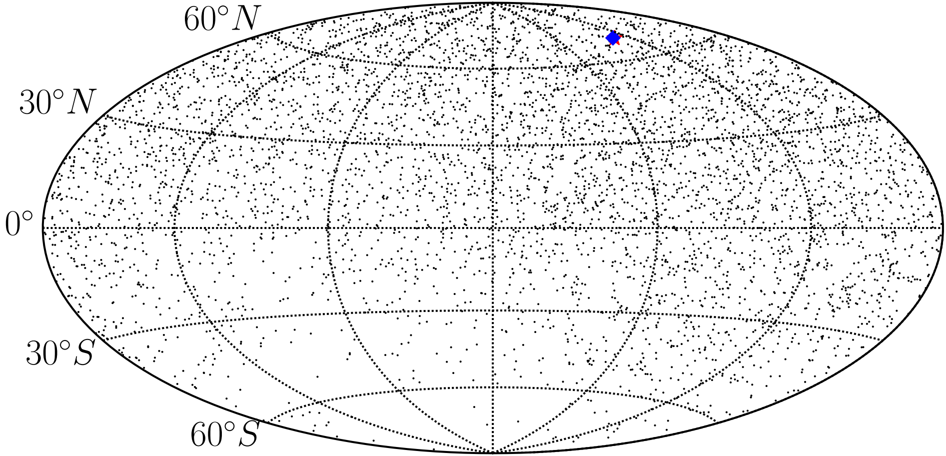

5000 events, $\alpha_D = 1$.
$\theta = 0.3^\circ$, $\Delta\alpha_D = 0.03$.

Sample Quadrupole

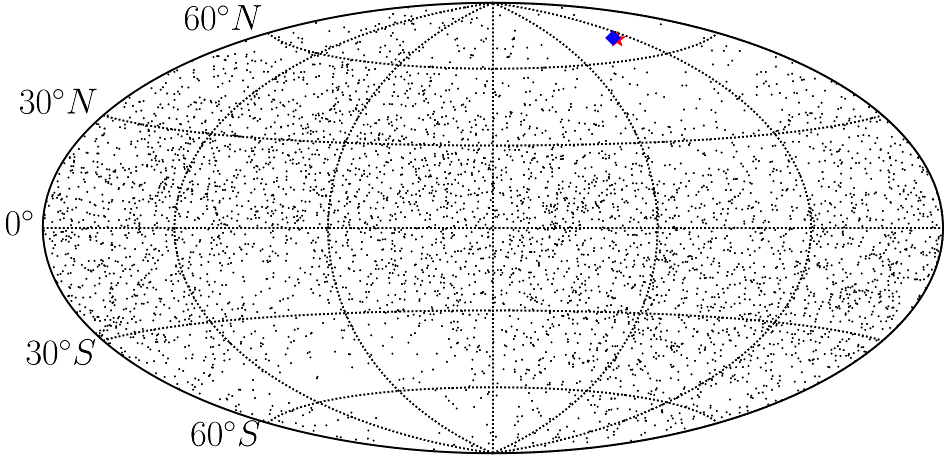

5000 events, $\alpha_Q = 1$.
$\theta = 0.8^\circ$, $\Delta\alpha_Q = 0.02$.

2MRS Sky Map

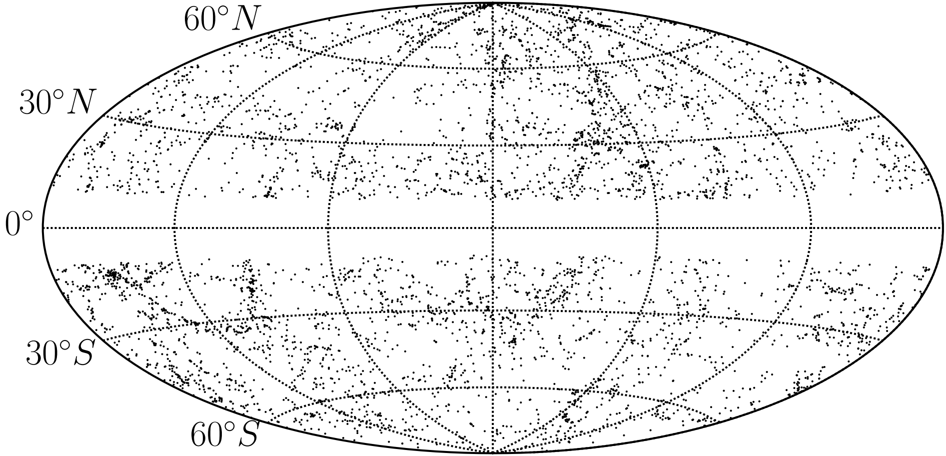

2MRS: 1108.0669

Spherical Harmonics: Possible Sources

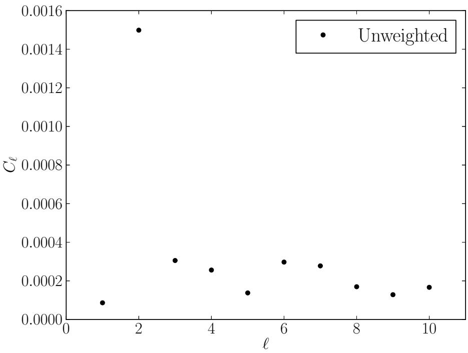

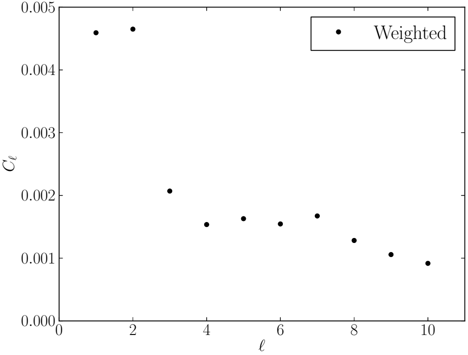

Auger's Nonuniform Partial Sky Coverage

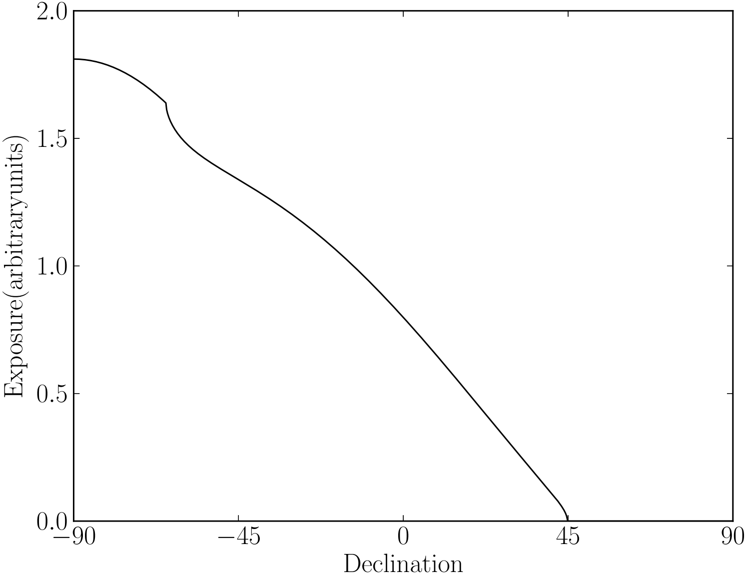

Reconstructing a_ℓ^m's for Nonuniform Partial Sky Coverage

Nonuniform exposure is a manageable problem:

$$\bar{a}_\ell^m = \frac{1}{N}\sum_i^N Y_\ell^{m*}(\Omega_i)$$

Reconstructing a_ℓ^m's for Nonuniform Partial Sky Coverage

Nonuniform exposure is a manageable problem:

$$\bar{a}_\ell^m = \frac{1}{N}\sum_i^N Y_\ell^{m*}(\Omega_i) \to \frac{1}{\mathcal{N}}\sum_i^N \frac{Y_\ell^{m*}(\Omega_i)}{\omega(\Omega_i)}\,,$$

where $\mathcal{N} = \sum_i^N \frac{1}{\omega(\Omega_i)}$,
ω is the exposure function.

Sommers: astro-ph/0004016

Reconstructing a_ℓ^m's for Nonuniform Partial Sky Coverage

Nonuniform exposure is a manageable problem:

$$\bar{a}_\ell^m = \frac{1}{N}\sum_i^N Y_\ell^{m*}(\Omega_i) \to \frac{1}{\mathcal{N}}\sum_i^N \frac{Y_\ell^{m*}(\Omega_i)}{\omega(\Omega_i)}\,,$$

where $\mathcal{N} = \sum_i^N \frac{1}{\omega(\Omega_i)}$,
ω is the exposure function.

Sommers: astro-ph/0004016

Partial sky is more challenging: no information from part of the sky.

$$[K]_{\ell m}^{\ell' m'} \equiv \int d\Omega\,\omega(\Omega) Y_\ell^m(\Omega) Y_{\ell'}^{m'}(\Omega)$$

$$b_\ell^m = \sum_{\ell' m'} [K]_{\ell m}^{\ell' m'} a_{\ell'}^{m'} \quad \Rightarrow \quad a_\ell^m = \sum_{\ell' m'}^{\ell_{\max}} [K^{-1}]_{\ell m}^{\ell' m'} b_{\ell'}^{m'}$$

$b_\ell^m \to$ uncorrected (observed on earth),
$a_\ell^m \to$ nature's true anisotropy.

Billoir, Deligny: 0710.2290

Sample Dipole with Auger's Exposure

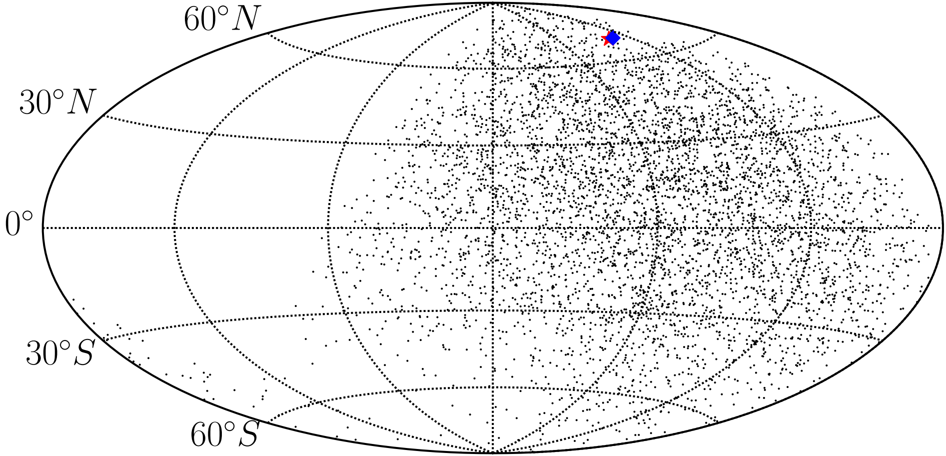

5000 events, $\alpha_D = 1$.
$\theta = 2^\circ$, $\Delta\alpha_D = 0.002$.

Dipole Reconstruction Effectiveness

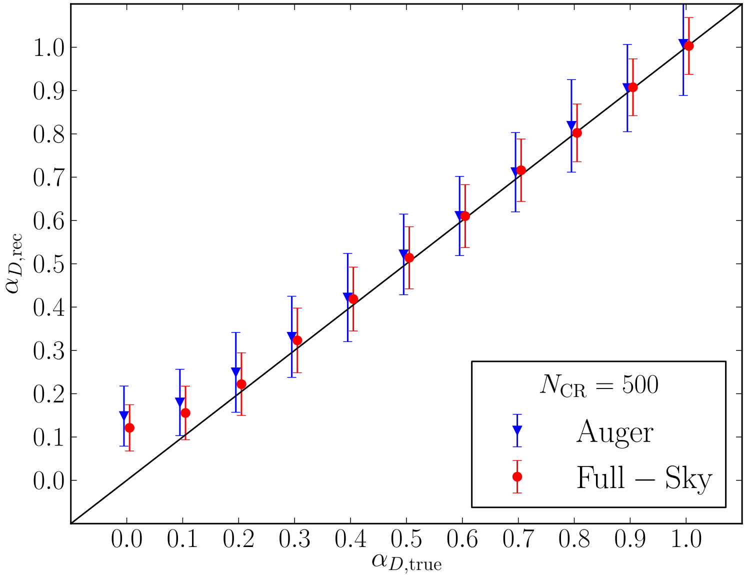

Reconstructing a_ℓ^m's for Nonuniform Partial Sky Coverage

- An alternative formalism to the K-matrix approach.
- Expand the exposure $\omega(\Omega)=\sum_{\ell,m}c_\ell^mY_\ell^m(\Omega)$.
- ω does not depend on RA $\Rightarrow$ only $m=0$ coefficients are nonzero.
- Fortuitously, $c_2^0=0$ for Auger's exposure
  (nearly equal to zero for Telescope Array).

Quadrupole Component of Exposure

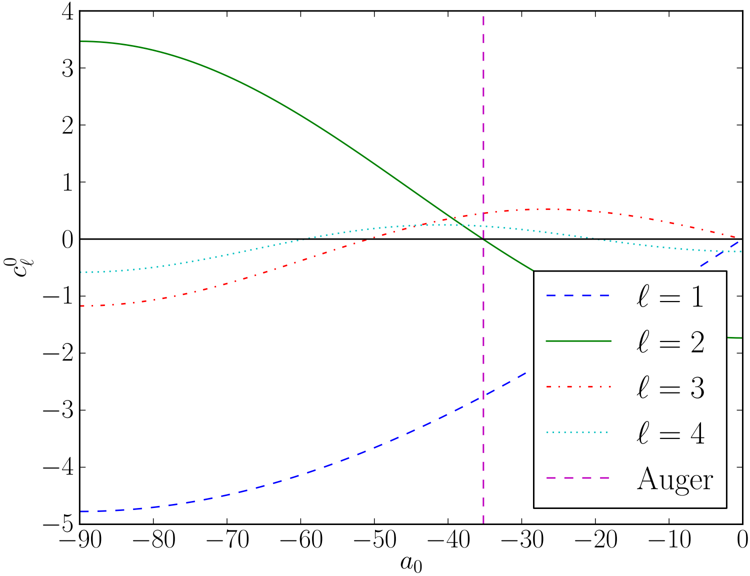

Reconstructing a_ℓ^m's for Nonuniform Partial Sky Coverage

When reconstructing a pure quadrupole, Auger and TA's exposures may be ignored,

$$b_2^m = a_2^m \left[1 + \frac{(-1)^m c_4^0 f(m)}{7\sqrt{4\pi}}\right]$$

A correction of $0.05, -0.04, 0.009$ for $|m| = 0, 1, 2$.

Sample Quadrupole with Auger's Exposure

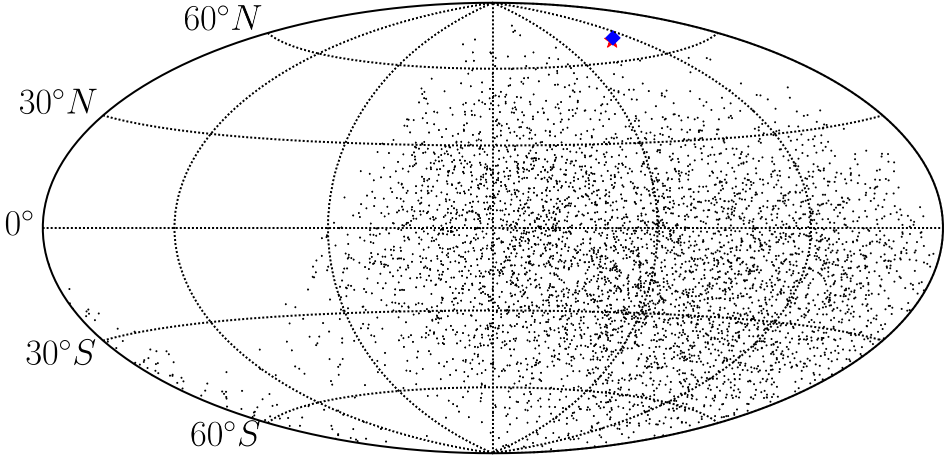

5000 events, $\alpha_Q = 1$.
$\theta = 2^\circ$, $\Delta\alpha_Q = 0.02$.

Quadrupole Reconstruction Effectiveness

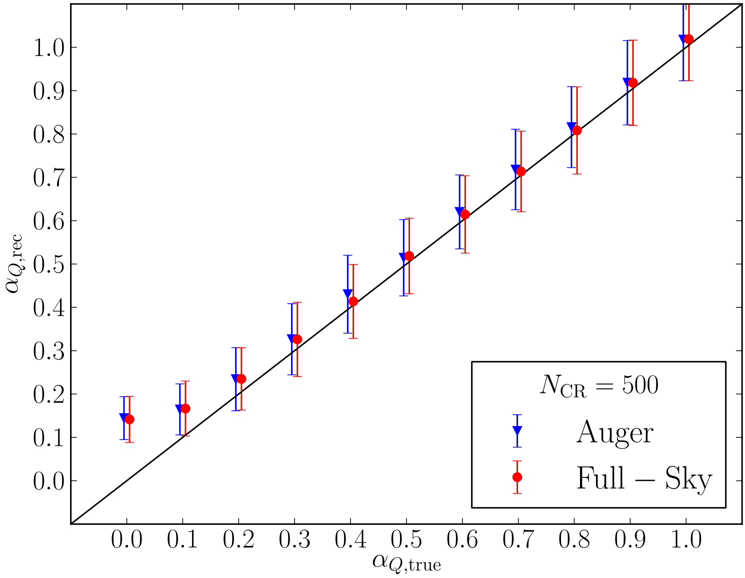

Conclusions

- The source(s) of UHECRs is still an open question.
- TA has evidence of a warm-spot.
- Auger and TA can reconstruct a quadrupole anisotropy without a partial sky penalty.
- In general, partial sky exposure $\Rightarrow$ anisotropy penalty factor.

Backups

About Integral Dispersion Relations: Subtraction

Cauchy + Integration Contour + Reflection Identities:

$$\Re f_+(E) = \frac{1}{\pi}\mathcal{P}\int_{m_p}^{\infty} dE' \Im f_+(E') \frac{2E'}{E'^2 - E^2}$$

$$\Re f_-(E) = \frac{1}{\pi}\mathcal{P}\int_{m_p}^{\infty} dE' \Im f_-(E') \frac{2E}{E'^2 - E^2}$$

The first integrand scales like $\sigma_{\rm tot}(E')$.

Integral won't converge and the outer circle $\not\to 0$.

Need a subtraction to reduce the power: add a pole.

$$\Re f_+(E) = \Re f_+(0) + \frac{1}{\pi}\mathcal{P}\int_{m_p}^{\infty} dE' \Im f_+(E') \frac{2E^2}{E'(E'^2 - E^2)}$$

New constant $f(0)$ - not physical.

Integral Dispersion Relations: Simple Cross Section

An analytic calculation requires several simplifications.

$$\sigma_{pp}(E) \to \sigma_0 \leftarrow \sigma_{p\bar{p}}(E)$$

$$m_p \to 0$$

Integral Dispersion Relations: Simple Cross Section

An analytic calculation requires several simplifications.

$$\sigma_{pp}(E) \to \sigma_0 \leftarrow \sigma_{p\bar{p}}(E)$$

$$m_p \to 0$$

Then,

$$\rho = \frac{2}{\pi}\mathcal{P}\int_0^\infty \frac{dx}{x^2-1} = 0$$

$$x \equiv E'/E.$$

Integral Dispersion Relations: Simple Cross Section

An analytic calculation requires several simplifications.

$$\sigma_{pp}(E) \to \sigma_0 \leftarrow \sigma_{p\bar{p}}(E)$$

$$m_p \to 0$$

Then,

$$\rho = \frac{2}{\pi}\mathcal{P}\int_0^\infty \frac{dx}{x^2-1} = 0$$

$$x \equiv E'/E.$$

Modifying the cross section with a step increase at $E'_{\rm min}, x_{\rm min}$,

$$\rho(x_{\rm min}) = \int_{x_{\rm min}}^\infty \frac{dx}{x^2-1} > 0$$

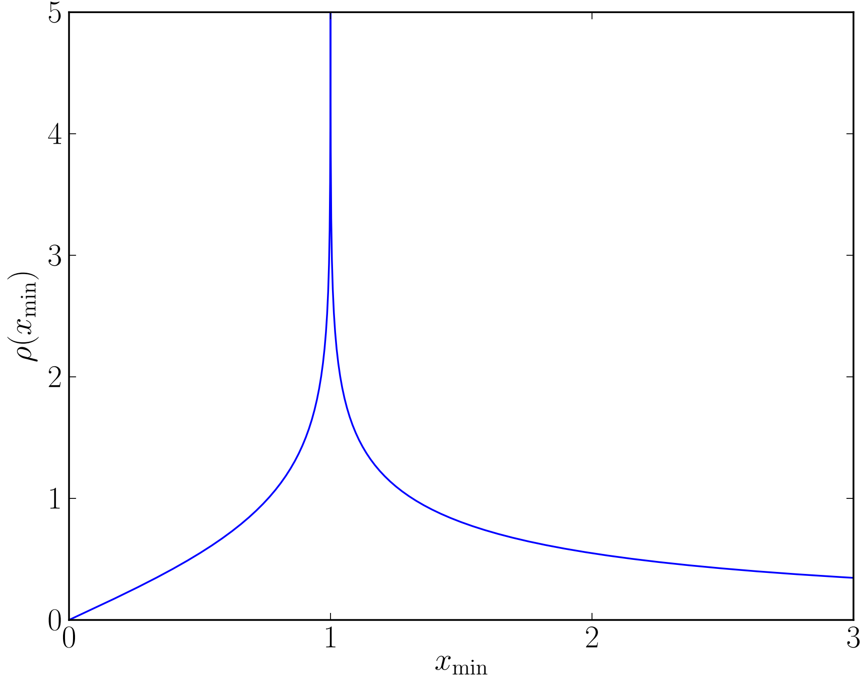
5
4
3
2
1
0
$\rho(x_{\min})$
0
1
2
3
$x_{\min}$

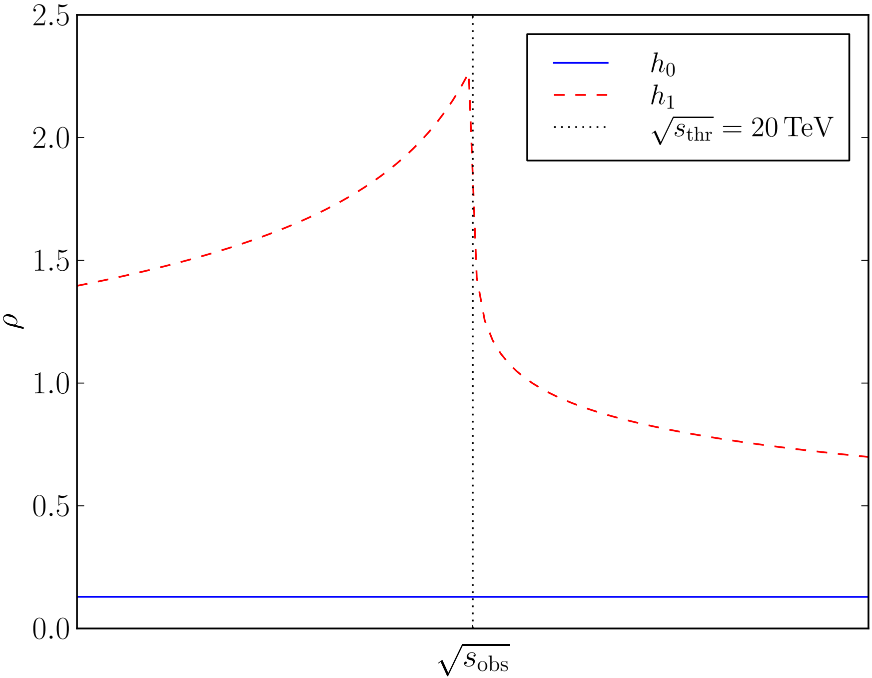
2.5
2.0
1.5
1.0
0.5
0.0
ρ
$\sqrt{s_{\rm obs}}$
h_0
h_1
$\sqrt{s_{\rm thr}} = 20\,{\rm TeV}$

Diffractive Cross Section Reproduces Froissart Bound

The cross section function that goes into the modification h_3 rises like $\log^2 s$ in the appropriate limit:

$$\sigma \propto 1 - \xi_p - \log \xi_p + \left(1 - \xi_p + \xi_p \log \xi_p + \frac{1}{2}\log^2 \xi_p\right)\epsilon + \mathcal{O}(\epsilon^2)$$

with higher order ϵ terms resulting in higher orders of $\log s$ following the above pattern.

Measuring ρ at the LHC

- Most cited values of ρ are calculated from IDRs.
- It is possible to measure ρ in a model independent fashion.

$$\frac{d\sigma}{dt} = \frac{\pi}{k^2}|f|^2 \qquad \frac{d\sigma}{dt} = \left.\frac{d\sigma}{dt}\right|_{t=0} e^{Bt}$$

B is the measured slope parameter, valid at low $|t|$.

$$\left.\frac{d\sigma}{dt}\right|_{t=0} = \frac{\pi}{k^2}\left|(\rho + i)\Im f(t=0)\right|^2 = \frac{\rho^2+1}{16\pi}\sigma_{\rm tot}^2$$

- Measuring $\sigma_{\rm tot}$ without ρ is difficult.
- Requires an accurate luminosity measurement.
- Moreover $\sigma_{\rm tot}$ only weakly depends on ρ.

What Anisotropies Can Do For Us

- Provide hints about the source(s),
- Can indicate composition and magnetic field strength,
- Can update models of acceleration.

Simple Anisotropy Measures

A general anisotropy measure:

$$\alpha \equiv \frac{I_{\max} - I_{\min}}{I_{\max} + I_{\min}} \in [0,1]\,.$$

Define

$$\alpha_D \equiv \sqrt{3}\frac{|a_1^0|}{a_0^0} \qquad\qquad \alpha_Q \equiv \frac{-3\sqrt{\frac{5}{4}}\frac{a_2^0}{a_0^0}}{2+\sqrt{\frac{5}{4}}\frac{a_2^0}{a_0^0}} \quad \text{('New' later)}\,,$$

Then $\alpha_D = \alpha$ for a purely dipolar distribution and $\alpha_Q = \alpha$ for a purely quadrupolar distribution.

Spherical Harmonics Visualizations

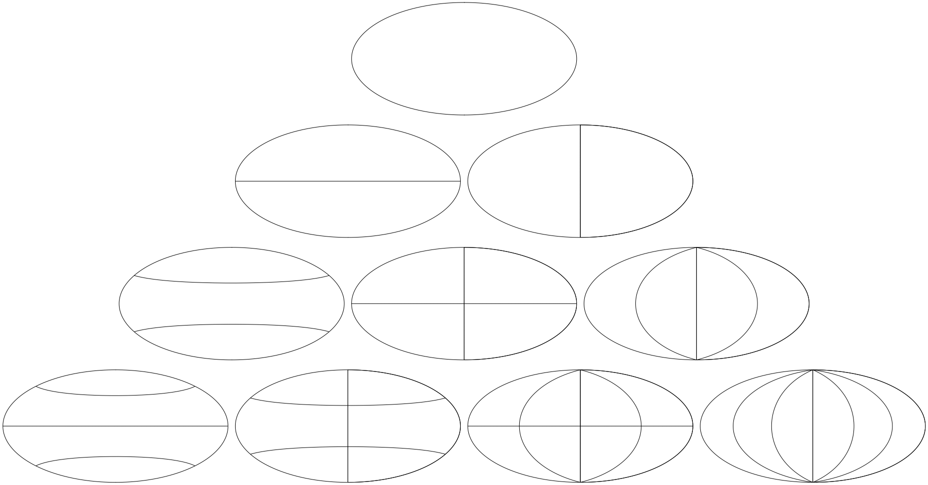

Spherical Harmonics: Possible Sources

Identifiable sources: Cen A, supergalactic plane, etc. use specific Y_ℓ^m's.

$$\begin{array}{lcll} \text{Point source} & \Rightarrow & \text{dipole:} & I_D \propto a_0^0 Y_0^0 + a_1^0 Y_1^0. \\ \text{Planar source} & \Rightarrow & \text{quadrupole:} & I_Q \propto a_0^0 Y_0^0 + a_2^0 Y_2^0. \end{array}$$

Each Y_ℓ^m partitions the sky into $\sim \ell^2/3$ zones, so $\ell_{\max} \approx \sqrt{3N}$.

Spherical Harmonic Coefficients: Galaxies

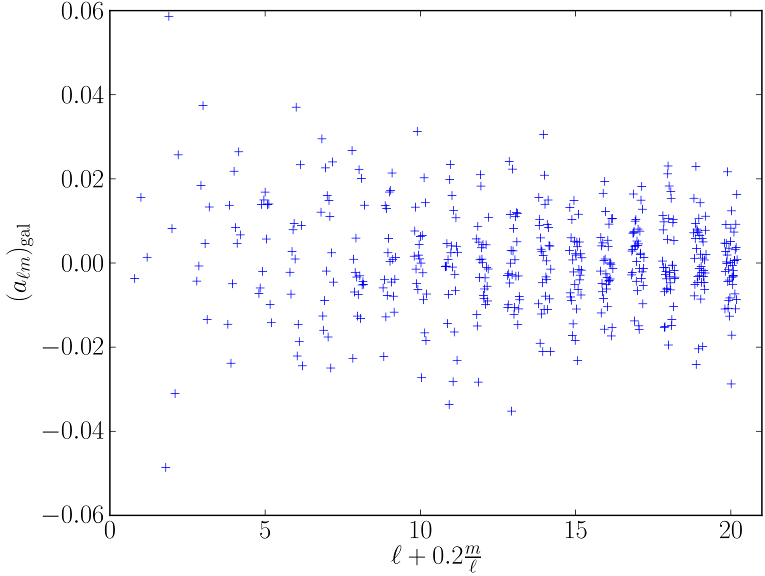

Spherical Harmonic Coefficients: Uniform

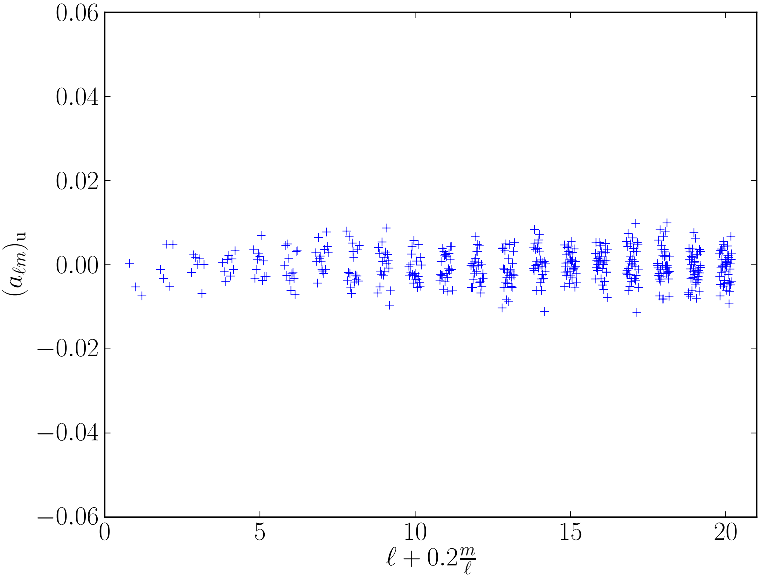

Catalogs

- We consider galactic catalogs.
- The catalog used is the 2MRS.
- Contains 5310 galaxies out to redshift 0.03: 120 Mpc.
- Nearby galaxies need their distances adjusted for peculiar velocities.

Quadrupole Component of Exposure

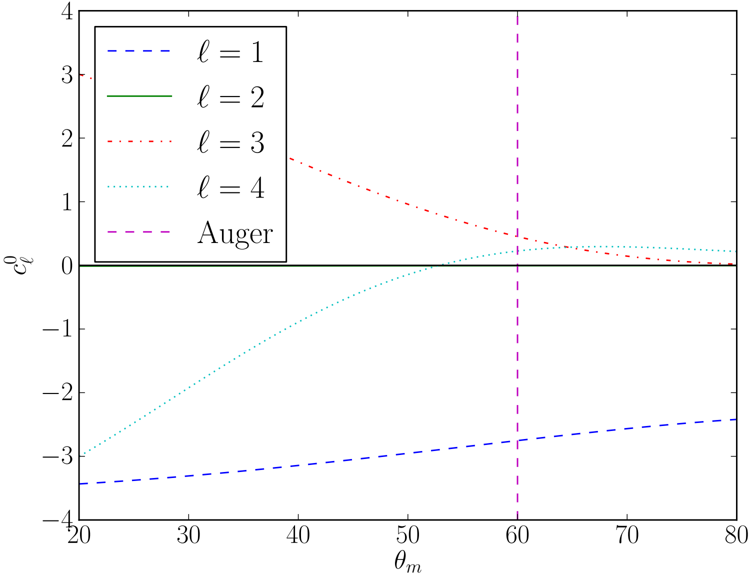

Quadrupole Reconstruction Technique Effectiveness

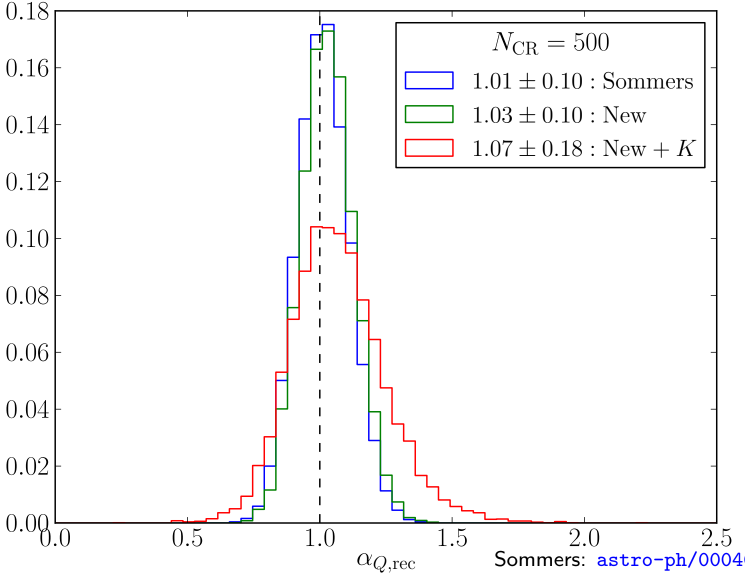

Sommers: astro-ph/0004016

Rotational Invariance of the Power Spectrum

$$I(\Omega) = \frac{1}{N}\sum_{i=1}^{N}\delta(\mathbf{u}_i,\Omega)\,,$$

$$\bar{a}_\ell^m = \frac{1}{N}\sum_{i=1}^{N}Y_\ell^{m*}(\mathbf{u}_i)\,,$$

$$\bar{C}_\ell = \frac{1}{N^2(2\ell+1)}\sum_{|m|\leq\ell}\left|\sum_{i=1}^{N}Y_\ell^{m*}(\mathbf{u}_i)\right|^2\,.$$

The addition formula for spherical harmonics:

$$P_\ell(\mathbf{x}\cdot\mathbf{y}) = \frac{4\pi}{2\ell+1}\sum_{|m|\leq\ell}Y_\ell^{m*}(\mathbf{x})Y_\ell^m(\mathbf{y})\,.$$

e.g. Arfken, Weber: *Mathematical Methods for Physicists*

$$\bar{C}_\ell = \frac{1}{4\pi N} + \frac{1}{2\pi N^2}\sum_{i<j}P_\ell(\mathbf{u}_i\cdot\mathbf{u}_j)\,.$$

b10-cut: Analytical Derivation

We conservatively fill in the unknown region of the galactic distribution with a uniform distribution,

$$I_g(\Omega) = I_{g,>10}(\Omega) + I_{u,<10}(\Omega)\,.$$

$$(a_\ell^m)_g = (a_\ell^m)_{g,>10} + (a_\ell^m)_{u,<10}\,,$$

Note the following properties of the $(a_\ell^m)_{u,<10}$:

- $I_{u,<10}$ isn't a function of ϕ.

$$a_\ell^m = 2\pi\sqrt{\frac{2\ell+1}{4\pi}}\int P_\ell(x)I(x)d(x)\delta_{m0}\,.$$

- $I_{u,<10}$ has even parity (the P_ℓ have definite parity).

$$(a_\ell^0)_{u,<10} = \sqrt{\frac{2\ell+1}{4\pi}}\int_0^{\cos(80^\circ)} P_\ell(x)dx\,.$$

b10-cut: Numerical Verification

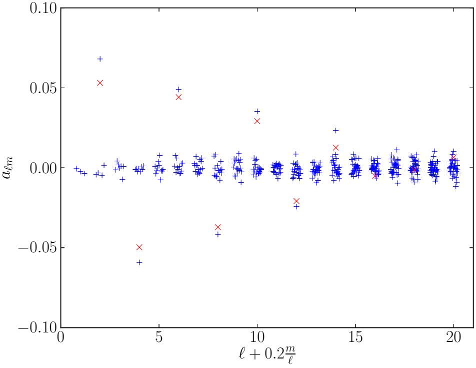

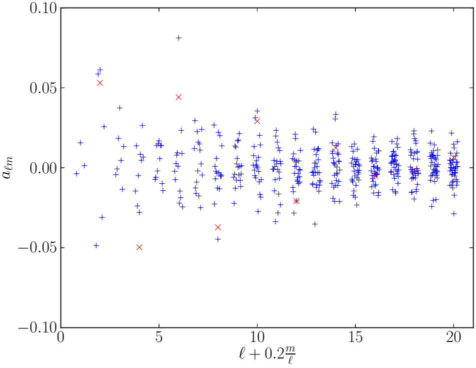

Uniform

2MRS